Journal of Power Sources 196 (2011) 2279–2282

Contents lists available at ScienceDirect

Journal of Power Sources

journal homepage: www.elsevier.com/locate/jpowsour

Short communication

$Li_3V_2(PO_4)_3$/C composite as an intercalation-type anode material for lithium-ion batteries

X.H. Rui, N. Yesibolati, C.H. Chen*

CAS Key Laboratory of Materials for Energy Conversion, Department of Materials Science and Engineering, University of Science and Technology of China, Anhui, Hefei 230026, China

ARTICLE INFO

Article history:
Received 28 May 2010
Received in revised form 3 September 2010
Accepted 14 September 2010
Available online 21 September 2010

Keywords:
Lithium vanadium phosphate
Lithium ion battery
Anode material
Intercalation

ABSTRACT

The carbon coated monoclinic $Li_3V_2(PO_4)_3$ (LVP/C) powder is successfully synthesized by a carbothermal reduction method using crystal sugar as the carbon source. Its structure and physicochemical properties are investigated using X-ray diffraction (XRD), scanning electron microscopy, high-resolution transmission electron microscopy and electrochemical methods. The LVP/C electrode exhibits stable reversible capacities of 203 and 102 mAh g^{-1} in the potential ranges of 3.0–0.0 V and 3.0–1.0 V versus Li^+/Li, respectively. It is identified that the insertion/extraction of Li^+ undergoes a series of two-phase transition processes between 3.0 and 1.6 V and a single phase process between 1.6 and 0.0 V. The ex situ XRD patterns of the electrodes at various lithiated states indicate that the monoclinic structure can still be retained during charge–discharge process and the insertion/deinsertion of lithium ions occur reversibly, which provides an excellent cycling stability with high energy efficiency.

1. Introduction

Rechargeable lithium-ion batteries have been considered as an attractive power source for a wide variety of applications, such as portable electronic products, electrical vehicles (EVs), hybrid electrical vehicles (HEVs). To meet the needs of these Li-ion battery technologies, phosphate polyanion materials based on either the ordered olivine (e.g. $LiFePO_4$) or NASICON (e.g. $Li_3V_2(PO_4)_3$) structures have been identified as promising high-safety cathode materials [1–4]. In particular, monoclinic lithium vanadium phosphate $Li_3V_2(PO_4)_3$ (LVP) has attracted much attention due to its higher specific capacity of up to 197 mAh g^{-1} and operating potential of up to 4.8 V [3,4]. The structure of monoclinic LVP (space group $P2_1/n$) is a three-dimensional framework of slightly distorted VO_6 octahedra and PO_4 tetrahedra linked together via common apical oxygens to form a $(V–O–P–O)_n$ bonding arrangement, which houses Li^+ ions in relatively large interstitial sites [4–7]. As a cathode material for lithium-ion batteries, all of Li^+ ions in the lattice can be reversibly extracted out and inserted back again with good ionic mobility [8–10]. Similar to $LiFePO_4$, however, the LVP suffers a problem of low intrinsic electronic conductivity, which inhibits its wide practical application. Fortunately, carbon coating is a proven simple way to improve its electronic conductivity, which is usually realized by introducing an organic precursor in the starting materials of the synthesis [8–10].

Kalaiselvi et al. in 2004 [11] and Ren et al. in 2010 [12] investigated respectively $LiFePO_4$ and β-$LiVOPO_4$ as possible anode materials for lithium-ion batteries. Although they have found that a reversible capacity of around 300 mAh g^{-1} can be measured for $LiFePO_4$ (3.3–0.0 V) and 380 mAh g^{-1} for β-$LiVOPO_4$ (3.5–0.0 V), their voltage profiles demonstrate a behavior of conversion reaction mechanism that leads to relatively low energy efficiency (less than 60%) and rather large initial capacity loss (35% for $LiFePO_4$ and 32% for β-$LiVOPO_4$). These results indicate that these two materials are not superior to many transition metal oxides such as CoO and Fe_3O_4 in terms of electrochemical properties.

Different from $LiFePO_4$ and β-$LiVOPO_4$, the monoclinic LVP has a more open structure; the theoretical density is 3.65, 3.27 and 3.04 g cm^{-3} for $LiFePO_4$, β-$LiVOPO_4$, and LVP, respectively. Therefore, it is possible that Li^+ ions can insert into the lattice of LVP without causing too much structure change and hence proceed in an intercalation reaction mechanism. The study described in this communication has confirmed this idea. Also, by introducing the carbon coating in the LVP/C composite, excellent cycling stability can be achieved, suggesting that LVP/C is a very promising high-safety anode material.

2. Experimental

The carbon coated monoclinic $Li_3V_2(PO_4)_3$ was synthesized by a carbothermal reduction method. Stoichiometric amounts of Li_2CO_3, V_2O_5 and $NH_4H_2PO_4$ were dispersed into acetone along with 40 wt% crystal sugar, and then the mixture was ball milled (rotating speed: around 200 r min^{-1}) for 2 days to ensure intimate

* Corresponding author. Tel.: +86 551 3606971; fax: +86 551 3601592.
E-mail address: cchchen@ustc.edu.cn (C.H. Chen).

0378-7753/$ – see front matter © 2010 Elsevier B.V. All rights reserved.
doi:10.1016/j.jpowsour.2010.09.024

and homogenous mixing. The added crystal sugar acted as a carbon source that can not only reduce V^{5+} to V^{3+} but also form a continuous network structure of carbon for electronic conduction. After the ball milling, the mixture was dried at 70 °C in an oven to evaporate acetone and then preheated at 350 °C in N_2 atmosphere for 5 h to expel H_2O and NH_3. Finally, the precursor was reground and sintered at 750 °C for 16 h under flowing N_2 to yield the $Li_3V_2(PO_4)_3$/C composite. The residual carbon content in the LVP/C composite is calculated as about 12.0 wt% based on the weight variation of LVP/C after its oxidation in air at 600 °C. The methodology of this residual carbon measurement will be given elsewhere.

The structural analysis of the LVP/C composite was performed by the X-ray diffraction (XRD) using a rotating anode X-ray diffractometer (MXPAHF, Cu Kα radiation) in the 2θ range from 10° to 60° at a scan rate of 8° min^{-1}. And the ex situ XRD patterns of LVP/C electrode at various discharge states were obtained using a TTR-III theta/theta rotating anode X-ray diffractometer (Cu Kα radiation) with a low scan rate of 2° min^{-1} in the 2θ range of 10–60°. The morphology of the LVP/C composite was observed under a scanning electron microscope (SEM, JSM-6390LA) and its microstructure was examined using a high-resolution transmission electron microscope (HRTEM, JEOL-2010).

Electrochemical characterization was carried out with coin-type cells assembled in an argon-filled glovebox. For preparing working electrodes, a mixture of LVP/C, acetylene black, and poly(vinyl difluoride) (PVDF) at a weight ratio of 80:10:10 was pasted on a Cu foil. Lithium foil was used as counter electrode. The electrolyte consisted of a solution of 1 M $LiPF_6$ in ethylene carbonate (EC)/dimethyl carbonate (DMC) (1:1, w/w). The cells were tested on a multi-channel battery test system (NEWARE BTS-610) with galvanostatic charge and discharge in the voltage ranges of 3.0–0.0 V and 3.0–1.0 V.

3. Results and discussions

Fig. 1a shows the XRD pattern of the pristine LVP/C composite. All the peaks correspond to a single phase and can be indexed as monoclinic structure with space group $P2_1/n$. On the other hand, there is no evidence of diffraction peaks from carbon, which indicates that the residual carbon is with an amorphous structure and/or the thickness of the residual carbon on the LVP/C particles is too thin [13], and its presence does not influence the structure of LVP. The grain size, D, was calculated using the Scherrer's equation: $D = 0.9\lambda/(\beta \cos\theta)$, where λ is the X-ray wavelength and β is the full-width-at-half-maximum of the diffraction peak on a 2θ scale. Based

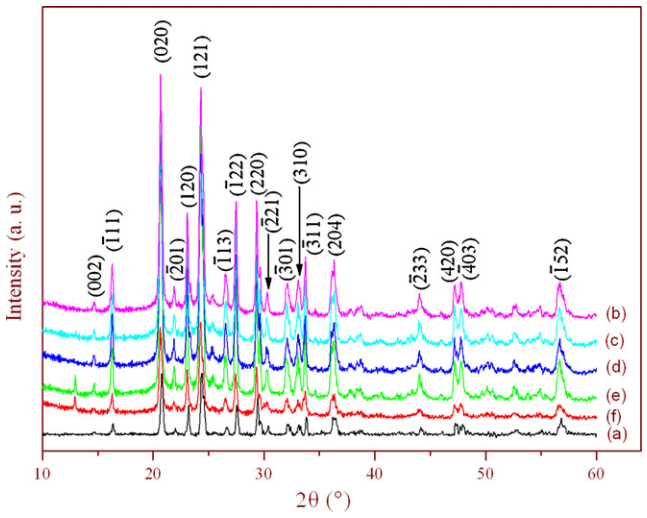

Fig. 1. XRD patterns of the LVP/C anode: (a) pristine LVP/C composite, and at potentials in the first discharge process: (b) 1.9 V, (c) 1.8 V, (d) 1.7 V, and (e) 1.6 V. The pattern (f) corresponds to and the LVP/C at the end of the second discharge process (0.0 V).

on diffraction planes of (1 2 1), (0 2 0) and (2 2 0), the mean value of grain size of LVP is 42 nm.

The SEM image of the LVP/C composite (Fig. 2a) displays an agglomerated morphology with a particle size of about 5–8 μm. The particles are composed of many intertwined flake-shaped microstructures, which are considered to be porous. This morphology is beneficial to the infiltration of electrolyte and to keep a large contact area between the electrolyte and the electrode. The presence of amorphous carbon layer is well illustrated in the HRTEM picture (Fig. 2b). The LVP crystallites appear in the darker regions, while the irregular-shaped carbon coating surrounds the primary particles of LVP.

At a current density of 0.013 mA cm^{-2}, the charge–discharge profiles of a LVP/C||Li half-cell in the voltage range of 3.0–0.0 V are shown in Fig. 3a. Four plateaus at around 1.95, 1.86, 1.74 and 1.66 V during the first discharge process are observed. They should correspond to a sequence of phase transition processes and the capacity at each plateau is about 30 mAh g^{-1}. Moreover, these four plateaus can also be seen on the subsequent charge–discharge curves, implying that these phase transition processes are reversible. Then, when the cell is further discharged from 1.6 V to 0.0 V, a sloping pro-

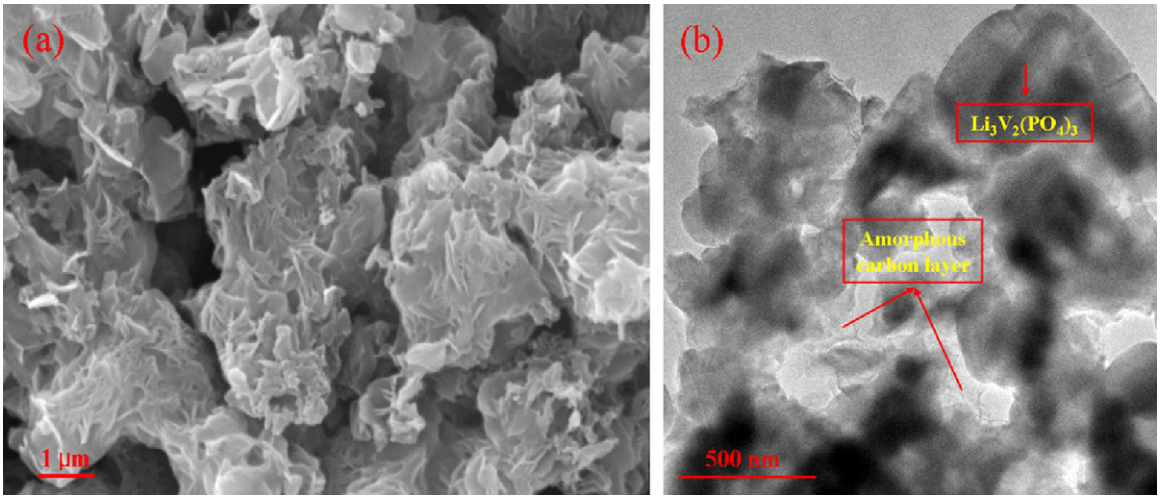

Fig. 2. SEM (a) and HRTEM (b) micrographs of the LVP/C composite.

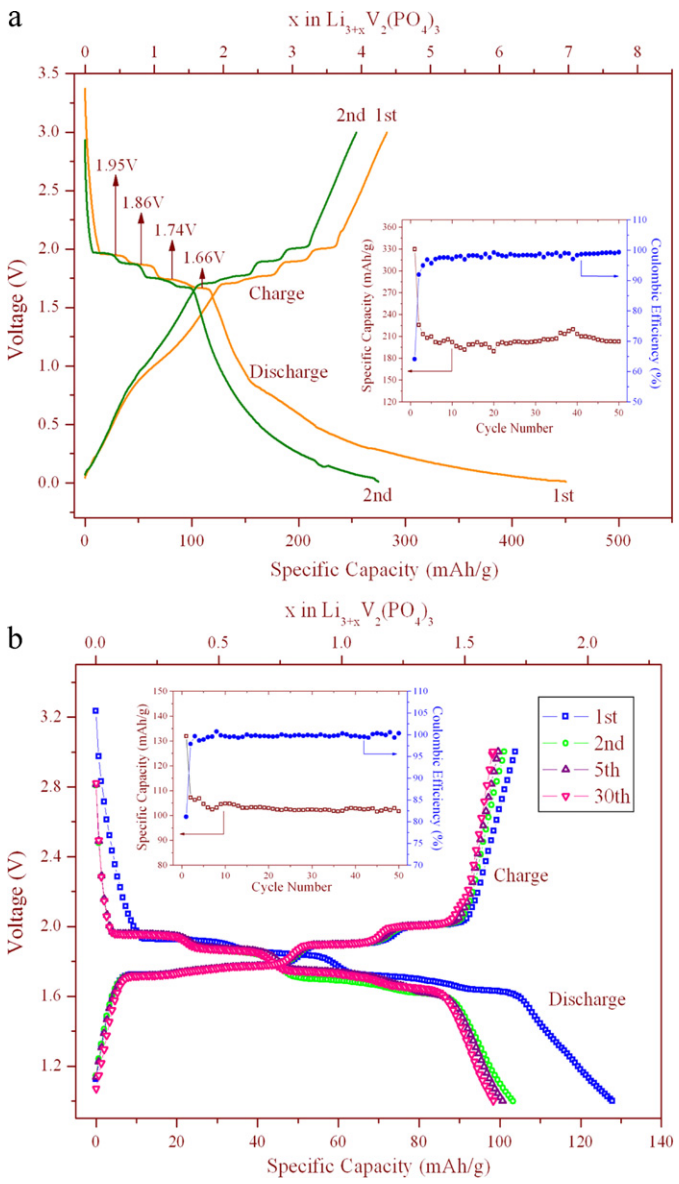

Fig. 3. Galvanostatic charge–discharge profiles of the LVP/C composite at a current density of 0.013 mA cm^{-2} in the voltage region of 3.0–0.0 V (a) and 3.0–1.0 V (b). Insets are their cycling performance at a current density of 0.1 mA cm^{-2}.

file is measured, indicating a solid solution behavior (i.e. single phase region). Obviously, as an anode material, the LVP/C composite shows an initial charge and discharge capacities of 282.9 and 450.3 mAh g^{-1}, respectively, which are much higher than the corresponding capacity values of the LVP/C cathodes [8–10]. The irreversible capacity loss (167.4 mAh g^{-1}) can be attributed to the formation of the solid electrolyte interphase (SEI) film on LVP as well as on both the above-mentioned amorphous carbon and acetylene black [12]. In the second cycle, the charge and discharge capacities are 254.3 and 274.8 mAh g^{-1}, respectively, displaying a largely reduced irreversible capacity loss (20.5 mAh g^{-1}). At a higher current density of 0.1 mA cm^{-2} (inset of Fig. 3a), the discharge capacities for the 1st, 2nd, 5th, 30th and 50th cycles are 329.8, 225.7, 209.7, 202.9 and 202.9 mAh g^{-1}, respectively, and the discharge capacity retention rate is over 90% from the 2nd to the 50th cycle. In addition, the coulombic efficiency is 64.1% for the first cycle and close to 100% upon progressive cycling.

It should be noted that the above capacity values are based on the total mass of LVP/C composite (i.e. 88 wt% LVP and 12 wt% residual amorphous carbon). We have evaluated the capacity of such residual carbon by dissolving the LVP/C composite in nitric acid and separating C for electrochemical measurement. The amorphous carbon gives a stable reversible capacity of 230 mAh g^{-1} between 1.5 and 0.0 V. The detailed study for the carbon evaluation will be given elsewhere. In addition, the conducting additive acetylene black in the electrode can also contribute a reversible capacity of 150 mAh g^{-1} between 1.5 and 0.0 V [14]. After taking all of these factors into account, we can recalculate the quantities of lithium insertion and extraction in LVP. If one lithium ion is inserted into a formula of $Li_3V_2(PO_4)_3$, the corresponding theoretical capacity can be calculated as 66 mAh g^{-1}. Noting that, when LVP is used as the cathode material, there are a sequence of phase transition processes in the voltage range of 3.0–4.8 V between the single phases $Li_xV_2(PO_4)_3$ (x = 3.0, 2.5, 2.0, 1.0 and 0) in the charge process. On the other hand, during the discharge process, it shows initially a solid solution behavior corresponding to two lithium insertion, and then two-phase behavior takes place at around 3.65 V ($Li_2V_2(PO_4)_3 \rightarrow Li_{2.5}V_2(PO_4)_3$) and 3.55 V ($Li_{2.5}V_2(PO_4)_3 \rightarrow Li_3V_2(PO_4)_3$). Similar to the LVP cathode, therefore, based on the voltage profiles at the low current density of 0.013 mA cm^{-2} and magnitude of capacities as well as ex situ XRD results of the lithiated LVP products (as shown below), the whole lithium insertion process of LVP anode is comprised of four consecutive two-phase regions followed by a single phase region, i.e. (1) approximately 0.5 Li^+ is inserted at every potential plateau around 1.95, 1.86, 1.74 and 1.66 V, corresponding to the composition changes $Li_3V_2(PO_4)_3 \rightarrow Li_{3.5}V_2(PO_4)_3 \rightarrow Li_4V_2(PO_4)_3 \rightarrow Li_{4.5}V_2(PO_4)_3 \rightarrow Li_5V_2(PO_4)_3$; (2) the single phase region between 1.6 V and 0.0 V corresponding to 2 Li^+ insertion from $Li_5V_2(PO_4)_3$ to $Li_7V_2(PO_4)_3$, being associated with the V^{2+}/V^+ redox couple.

Furthermore, the electrochemical performance of the LVP/C in the two-phase regions (between 3.0 V and 1.0 V) at a current density of 0.1 mA cm^{-2} is illustrated in Fig. 3b. As discussed above, four plateaus associated with the V^{3+}/V^{2+} redox couple correspond to a total of approximately two Li^+ insertion/deinsertion. The LVP/C gives rise to an initial charge and discharge capacities of 103.8 and 127.9 mAh g^{-1}, respectively, showing an irreversible capacity loss of 24.1 mAh g^{-1} and coulombic efficiency of 81.2%, which are much better than that in the voltage range of 3.0–0.0 V. Interestingly, the LVP/C in this voltage range possess an excellent cyclic reversibility with almost no capacity fading from the 2nd to the 50th cycle (inset of Fig. 3b). Also, the coulombic efficiency is near 100% after the second cycle. Patoux et al. has reported that a rapid capacity fade occurs in this voltage range due to vanadium dissolution into the electrolyte [15]. The excellent cycling in both narrow (3.0–1.0 V) and wide (3.0–0.0 V) voltage ranges achieved in this study may be attributed to the effect of carbon coating in the LVP/C composite that can prevent the direct contact between LVP particles and the electrolyte and hence minimize the vanadium dissolution.

In order to elucidate the structural changes during cycling, ex situ XRD measurements were carried out. Fig. 1b–f shows five ex situ XRD patterns of the LVP/C at various first discharged states of 1.9, 1.8, 1.7 and 1.6 V as well as at the end of the second discharged state (0.0 V). It can be seen that all the lithiated LVP products are isotypic with LVP (space group $P2_1/n$), which means that the monoclinic structure of LVP is very stable and the insertion/deinsertion of lithium ions can proceed reversibly. For patterns b–e measured at each end of four plateaus (see Fig. 1b–e), there are not any obvious difference and peak broadening, indicating that microstructural defects or a nonuniform distribution of local strain do not exist [16,17]. On the other hand, the lattice parameters of samples b–e were calculated by the Unit Cell software using the least-square method, which is shown in Table 1. With increasing discharge depth (1.9 V → 1.6 V), the cell volume increases slightly

Table 1
Lattice parameters of the lithiated LVP samples.

Samples	a (Å)	b (Å)	c (Å)	β (°)	Cell volume (Å^3)
(b) 1.9 V	8.605(0)	8.585(0)	12.062(4)	89.977(9)	891.093(5)
(c) 1.8 V	8.610(0)	8.588(4)	12.052(9)	89.916(3)	891.262(5)
(d) 1.7 V	8.596(5)	8.593(1)	12.109(0)	90.252(2)	894.493(8)
(e) 1.6 V	8.610(3)	8.597(8)	12.133(8)	89.732(7)	898.248(6)

from 891.093(5) to 898.248(6) Å^3, thus, the corresponding to a volume increases by 0.8%, which is very small and implies an excellent cycling reversibility in the two-phase regions. In addition, an extra small peak at $2\theta = 13^\circ$ is observed on the patterns e and f, corresponding to the highly lithiated states $Li_5V_2(PO_4)_3$ and $Li_7V_2(PO_4)_3$. It may be due to some degree of possible oxidation of the samples when they were exposed in air during the XRD measurement. Our preliminary analysis on this impurity phase indicates that it is a lithium vanadium oxide $Li_{0.6}V_{1.67}O_{3.67}$ (JCPDS card no. 50-0230).

4. Conclusions

The LVP/C composite has been successfully synthesized by the carbothermal reduction method using crystal sugar as the carbon source. As an anode material, the LVP/C composite exhibits stable reversible capacities of 203 and 102 mAh g^{-1} in the voltage range of 3.0–0.0 V and 3.0–1.0 V, respectively. During the charge–discharge process, it undergoes a sequence of phase transition processes among four individual isotypic monoclinic phases $Li_xV_2(PO_4)_3$ ($x = 3.0$, 3.5, 4.0, 4.5 and 5.0) in the voltage range of 3.0–1.6 V and a solid solution $Li_{5+y}V_2(PO_4)_3$ ($y = 0$–2.0) in the voltage range of 1.6–0.0 V. Because of the very small volume change (less than 1%) and thus the excellent, the carbon coated LVP is a promising high safety anode material for lithium ion batteries.

Acknowledgments

This study was supported by National Science Foundation of China (grant no. 20971117 and 10979049) and Education Department of Anhui Province (grant no. KJ2009A142). We are also grateful to the Solar Energy Operation Plan of Academia Sinica.

References

[1] A.K. Padhi, K.S. Nanjundaswamy, J.B. Goodenough, J. Electrochem. Soc. 144 (1997) 1188.
[2] A. Yamada, S.C. Chung, J. Electrochem. Soc. 148 (2001) A960.
[3] M.Y. Saidi, J. Barker, H. Huang, J.L. Swoyer, G. Adamson, J. Power Sources 119–121 (2003) 266.
[4] H. Huang, S.C. Yin, T. Kerr, N. Taylor, L.F. Nazar, Adv. Mater. 14 (2002) 1525.
[5] S.C. Yin, H. Grondey, P. Strobel, M. Anne, L.F. Nazar, J. Am. Chem. Soc. 125 (2003) 10402.
[6] S.C. Yin, H. Grondey, P. Strobel, H. Huang, L.F. Nazar, J. Am. Chem. Soc. 125 (2003) 326.
[7] P. Fu, Y.M. Zhao, Y.Z. Dong, X.N. An, G.P. Shen, J. Power Sources 162 (2006) 651.
[8] X.H. Rui, C. Li, C.H. Chen, Electrochim. Acta 54 (2009) 3374.
[9] Q.Q. Chen, J.M. Wang, Z. Tang, W.C. He, H.B. Shao, J.Q. Zhang, Electrochim. Acta 52 (2007) 5251.
[10] C.X. Chang, J.F. Xiang, X.X. Shi, X.Y. Han, L.J. Yuan, J.T. Sun, Electrochim. Acta 53 (2008) 2232.
[11] N. Kalaiselvi, C.H. Doh, C.W. Park, S.I. Moon, M.S. Yun, Electrochem. Commun. 6 (2004) 1110.
[12] M.M. Ren, Z. Zhou, X.P. Gao, J. Appl. Electrochem. 40 (2010) 209.
[13] H.C. Shin, W.I. Cho, H. Jang, J. Power Sources 159 (2006) 1383.
[14] J.L. Shui, S.L. Zhang, W.L. Liu, Y. Yu, G.S. Jiang, S. Xie, C.F. Zhu, C.H. Chen, Electrochem. Commun. 6 (2004) 33.
[15] S. Patoux, C. Wurm, M. Morcrette, G. Rousse, C. Masquelier, J. Power Sources 119–121 (2003) 278.
[16] H.W. Liu, D.G. Tang, Mater. Chem. Phys. 114 (2009) 656.
[17] Y. Kim, J. Oh, T.G. Kim, B. Park, Appl. Phys. Lett. 78 (2001) 2363.